



Preparation of activated charcoal from *Acrocomia aculeata* for purification of pretreated crude glycerol

Sandro L. Barbosa¹ · Milton S. de Freitas¹ · Wallans T. P. dos Santos¹ · David Lee Nelson¹ · Maria Betânia de Freitas Marques¹ · Stanley I. Klein² · Giuliano C. Clososki³ · Franco J. Caires³ · Eduardo J. Nassar⁴ · Lucas D. Zanatta⁵ · Foster A. Agblevor⁶ · Carlos A. M. Afonso⁷ · Adriano C. Moraes Baroni⁸

Received: 28 February 2020 / Revised: 13 April 2020 / Accepted: 29 April 2020
© Springer-Verlag GmbH Germany, part of Springer Nature 2020

Abstract

Activated charcoal was prepared from *Acrocomia aculeata* (macaúba) endocarp by $ZnCl_2$ activation and then used for the adsorptive purification of pretreated crude glycerol (CG) containing pigments, such as β -carotene. The pretreatment of glycerol involved filtration of the K_3PO_4 formed by the addition of H_3PO_4 to the crude glycerol containing KOH. A mixture of 1.38:1 w/w of $ZnCl_2$:*Acrocomia aculeata* pulp was heated at 120 °C with stirring for 24 h. The mixture was activated by heating at 600 °C for 3 h. The activated charcoal was cooled to 25 °C, washed with a 1:1 mixture of methanol and water (100 mL) and heated at 150 °C for 2 h. The surface properties of the activated charcoal (surface area $627\text{ m}^2\text{ g}^{-1}$, pore volume $0.39\text{ m}^3\text{ g}^{-1}$, Bronsted sites $118.23\text{ }\mu\text{mol g}^{-1}$, and Lewis sites $104.86\text{ }\mu\text{mol g}^{-1}$) and the adsorption capacity for impurities in H_3PO_4 -pretreated crude glycerol were investigated. The activated charcoal exhibited the most suitable surface properties for the purification of pretreated crude glycerol, attaining a 95.99% glycerol concentration (by GC) using 10 g/L with gravity filtration through a column at room temperature over a 48-h period. The purified glycerol was characterized by GC/MS, 1H - and ^{13}C -NMR, and DSC and TG analyses. The activated charcoal was regenerated by washing with methanol and hexane and heating to 150 °C for 5 h. The activated charcoal could be re-used three times to remove all of the pigments before it was necessary to re-activate the charcoal by heating with $ZnCl_2$.

Keywords Endocarp pulp of *Acrocomia aculeata* · Microporous-mesoporous charcoal · Prepared charcoal · Purification of crude glycerol by adsorption

✉ Sandro L. Barbosa
sandro.barbosa@ufvjm.edu.br

Milton S. de Freitas
freitas.milton@hotmail.com

Wallans T. P. dos Santos
wallanst@yahoo.com.br

David Lee Nelson
dleenelson@gmail.com

Maria Betânia de Freitas Marques
betanialf@hotmail.com

Stanley I. Klein
stanleiklein@gmail.com

Giuliano C. Clososki
gclososki@yahoo.com.br

Franco J. Caires
fjcaires@usp.br

Eduardo J. Nassar
ejnassar@unifran.br

Lucas D. Zanatta
lucaszanatta@usp.br

Foster A. Agblevor
foster.agblevor@usu.edu

Carlos A. M. Afonso
carlosafonso@ff.ulisboa.pt

Adriano C. Moraes Baroni
adriano.baroni@ufms.br

Extended author information available on the last page of the article

1 Introduction

Glycerol is the principal by-product of fatty acid methyl ester (FAME) (“biodiesel”) synthesis obtained via transesterification of triglycerides from vegetable oils or animal fats [1]. Approximately 10% w/w of glycerol is generated from the production of biodiesel. Because of the increase in biodiesel production [2–4], it is necessary to search for alternatives for the use of the glycerol by-product. Thus, various methods have been used for the disposal or utilization of crude glycerol (CG), including direct combustion [5, 6], fertilizer [7, 8], animal feed [9, 10], anaerobic digestion feedstock [8, 11], thermo-chemical or biological conversion products of greater value [12–18], additives (oxygenated additives) in fuels [19], and as a solvent for organic reactions [20]. However, with the rapid expansion of the biodiesel industry, the market is now flooded with excess crude glycerol, and any increase in biodiesel production will significantly increase the quantity of glycerol above the current market demand and decrease its economic value. Thus, the discovery of new uses for the crude glycerol so as to maintain or increase its value can improve the cost effectiveness of biodiesel production.

The crude glycerol obtained from biodiesel production is not suitable for use in its traditional applications because of the presence of various contaminants, such as moisture, ash, soap, alcohol, traces of glycerides, and vegetable color, which results in a low glycerol content in the chromatography gas [21, 22]. Recently, various studies have focused on methods for the purification or enrichment of glycerol, such as simple vacuum distillation [23, 24], electrodialysis [25], ion-exchange chromatography [26, 27], membrane filtration [28], and chemical processes [29–32]. Adsorption is recognized as a generally efficient and economical process for the removal of organic compounds from an aqueous solution because of the low energy consumption, the ability to operate at ambient temperature and pressure, and the possibility of regenerating the spent adsorbent, in addition to the broad availability of adsorbents [33]. One such abundant and relatively cheap adsorbent is activated charcoal, which can be prepared by physical or chemical activation methods or by a combination of both [34]. Chemical activation uses dehydrating agents that influence the pyrolytic decomposition, inhibit tar formation, and enhance the yield of charcoal [35]. In addition, the temperatures used in chemical activation are lower than those used in the physical activation process, resulting in the development of a better porous structure and catalytic activity than that obtained from the physical activation process [36]. Chemical activation of various types of carbonaceous materials, such as coal-tar pitch, biomass, and industrial and domestic wastes, typically employs alkali, such as KOH [32, 34–36] or NaOH [37, 38], and some Bronsted (HNO_3 [39] and H_3PO_4 [40–42]) and Lewis acids, such as ZnCl_2 [43–45], as activators. In this paper, activated charcoal was prepared

from the endocarp of *Acrocomia aculeata* (macaúba) using ZnCl_2 activation, and the product was evaluated for the production of a purified glycerol with a purity greater than the limit established by the BS 2621 standard (specifications for glycerol) (C 80% (w/w)). *Acrocomia aculeata* is a plant that is native to Brazil, widely distributed and easily accessible. The endocarp of the fruit has a high oil content, and the residue from the plant can be used to produce charcoal.

2 Experimental

2.1 Raw materials and chemicals

Crude glycerol was obtained from the transesterification of waste cooking oil, obtained from local restaurants, with methanol using KOH as the catalyst, as described by Komintarachat and Chuepeng [46]. Acetone, zinc chloride, sodium carbonate, commercial activated charcoal, and concentrated sulfuric and phosphoric acids from VETEC were used as purchased.

2.2 Analysis of feedstock and products

Purified glycerol content and yields were determined on a Shimadzu GC/MS-QP5050. Gas chromatograph/mass spectrometer equipped with an AOC-20i auto injector and an NA-WAX (30 m \times 0.25 mm; 0.25 μm film thickness) column. Direct insertion spectra were measured by electron impact at 70 eV; injector temperature, 250 $^\circ\text{C}$; interface temperature, 250 $^\circ\text{C}$; split ratio, 100; temperature program, isotherm at 50 $^\circ\text{C}$ for 2 min; followed by an increase of 10 $^\circ\text{C min}^{-1}$ to 230 $^\circ\text{C}$, where the temperature was maintained for 15 min. The carrier gas was helium with a flow rate of 1.1 mL min^{-1} . The volume injected was 1.0 μL . MS acquisition rate is 45 m/z at 550 m/z from 10 to 35 min. ^1H - and ^{13}C -NMR spectra were recorded on Bruker Avance 400 Spectrometers. The refractive indices of the samples were measured on a Reichert ABBE Mark II refractometer.

The DSC curves were obtained in the Shimadzu DSC60 cell, calibrated with indium ($T_{\text{onset}} = 156.63$ $^\circ\text{C}$, $\Delta H_{\text{fus}} = 28.45$ J/g) under a dynamic nitrogen atmosphere with a flow rate of 50 mL/min , a heating rate of 10 $^\circ\text{C/min}$ from 30 to 400 $^\circ\text{C}$ in a closed aluminum crucible, and a sample mass of 1.5 mg were used. The temperature indicative of the phenomenon is defined by T_{onset} ($^\circ\text{C}$) and enthalpy (ΔH) or transition energy, expressed in J/g . The thermal gravimetric (TG) curves were obtained on the Shimadzu DTG60 thermobalance with a heating rate at 10 $^\circ\text{C/min}$ from 30 to 600 $^\circ\text{C}$ under a dynamic nitrogen atmosphere with a flow rate of 50 mL/min . An aluminum crucible and sample mass of approximately 2.5 mg were used.

2.3 Treatment methods

2.3.1 Pretreatment of crude glycerol using H_3PO_4

Purification of crude glycerol was performed using a combination of chemical and physical treatments with solvent extraction, as described by the literature [18, 19, 28]. A 200-mL portion of crude glycerol was obtained from the transesterification of waste cooking oil with methanol using KOH as the catalyst [47]. The methanol from the transesterification process was evaporated with the aid of a rotary evaporator, and the crude glycerol residue (135.10 g) was pretreated by the addition of H_3PO_4 (85%) to a pH of 2, followed by shaking for 1 h at a constant rate of 200 rpm and allowing to stand for 12 h for phase separation by decantation. The top layer contained FAME, fatty acids, and soap; the middle layer was rich in glycerol; and the bottom layer contained a salt-rich solid (K_3PO_4) which was filtered. The liquid mixture was transferred to a separation funnel, the upper phase was separated, and the intermediate glycerol phase was neutralized by the addition of KOH pellets to pH 7.0, centrifuged to remove the salt and extracted with propanol; the solvent was separated from glycerol using a rotary evaporator. All the experiments were performed in triplicate.

2.3.2 Preparation and activation of charcoal from *Acrocomia aculeata*

The raw material used for preparing the activated charcoal was the endocarp of the macaúba fruit from the American palm tree *Acrocomia aculeata*. The vegetable oil contained in the macaúba fruit was extracted into hexane from a 100-g portion of fruit using 100 mL of hexane. The mixture (fruit and hexane) was stirred with a mechanical stirrer at a constant rate of 200 rpm for 1 h at room temperature and filtered. The solid residue of the fruit was dried in an oven at 150 °C for 2 h. Finally, the fruit residue was ground in an industrial blender and sifted through an 80-mesh sieve to yield a size range of 1–2 mm. The preparation of the activated charcoal from *Acrocomia aculeata* endocarp was performed in the two main steps of pyrolysis and activation. For the pyrolysis step, approximately 50 g of the sifted fruit residue was mixed with 70 g of $ZnCl_2$ and heated at 600 °C in a muffle furnace for 2 h before being cooled slowly to room temperature. The sample was crushed and sifted to obtain a size smaller than 0.25 mm. Ready-to-use charcoal was obtained after washing with 100 mL of deionized water and 100 mL of methanol to constant pH and drying at 150 °C for 2 h. The textural properties of activated charcoal obtained from *Acrocomia aculeata* endocarp were measured with a surface area analyzer using the Brunauer-Emmett-Teller (BET) method. All the experiments were performed in triplicate.

2.3.3 Acidity of prepared and commercial activated charcoals

Quantification of the Brønsted and Lewis acid sites was performed by pyridine absorption spectroscopy. The spectra were recorded on a Perkin Elmer Frontier spectrometer using the KBr pellet method with known mass. Samples of commercial charcoals and the charcoal prepared in the laboratory from the macaúba pulp were dried for 2 h at 120 °C. The pellet, after having its spectrum recorded in the infrared region, was stored in a desiccator in the presence of 2.0 mL of pyridine for 1 h. The infrared spectrum was recorded, all the measurements being performed at room temperature.

2.3.4 Purification of the pretreated crude glycerol

The adsorptive purification of the pretreated crude glycerol was carried out at room temperature (25 °C) and ambient pressure using a column (15.0 cm height by 1.0 cm diameter) containing the activated charcoal (10 g). Small aliquots of crude pretreated glycerol were added to the column until a total volume of 1 L of glycerol was added. The adsorption lasted 48 h. The purity of the filtered glycerol was determined by GC/MS, 1H - and ^{13}C -NMR, and DSC and TG analyses. The regeneration of used activated charcoal was performed after shaking at 250 rpm with methanol in the ratio of 3:1 (v/w) for 1 h to remove the adsorbed glycerol. The activated charcoal was separated from the solution by filtration, rinsed with hexane to remove the excess solvent, and heated in a muffle furnace at 150 °C for 5 h for reactivation. After using the charcoal three times, it no longer retained all of the pigments and required reactivation by heating with $ZnCl_2$.

3 Results and discussion

3.1 Characterization of prepared and commercial activated charcoal

The pretreatment of the crude glycerol was performed with concentrated sulfuric and phosphoric acids. However, the results of the treatment with sulfuric acid were inferior (75.85% purity), so only treatment with H_3PO_4 was used to yield glycerol of 95.99% purity. This result is similar to that obtained by Manusak et al. [19]. In addition to the fact that K_2SO_4 is slightly soluble in glycerol, H_2SO_4 is a much stronger acid than H_3PO_4 and can catalyze side reactions of glycerol [18]. The refractive index of the purified glycerol was 1.4600 (Glycerol standard (Sigma-Aldrich), 1.4704). The remaining 4.01% is probably water.

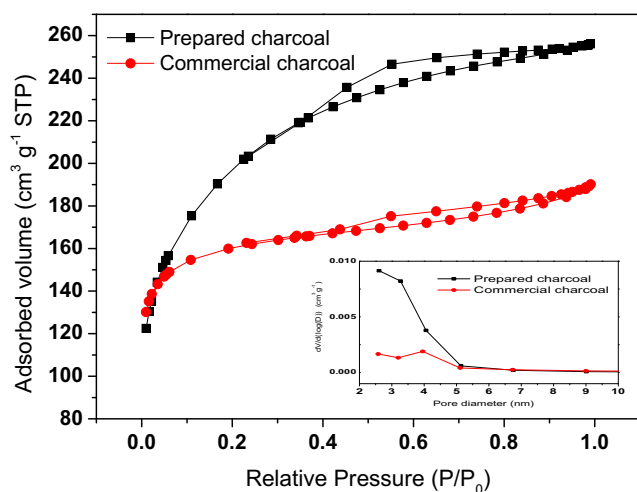


Fig. 1 Nitrogen adsorption and desorption isotherms of prepared and commercial charcoals

3.1.1 Nitrogen adsorption

Hysteresis in the isotherms, characteristic of capillary condensation phenomena, and typical of materials containing mesopores [48], was observed for the prepared and commercial charcoals. In fact, the textural properties such as the surface area and

porosity of adsorbents have a great influence on the adsorption properties, because some factors combined with surface chemistry govern the free energy of adsorption of the crude pretreated glycerol [49]. A careful analysis of these textural properties is needed because a larger mesoporous presence in the adsorbent can favor mass transportation, whereas a large presence of micropores can result in a constrains to the diffusion process. Because of the behavior of the isotherms, we clearly noted the large presence of micropores in both adsorbents, as is evidenced in the low pressure regions (Fig. 1). The prepared charcoal had a larger total specific surface area ($S_{\text{BET}} = 627 \text{ m}^2 \text{ g}^{-1}$) than that of the commercial charcoal ($S_{\text{BET}} = 470 \text{ m}^2 \text{ g}^{-1}$). In addition, 73% of the total area in the commercial charcoal was microporous area ($S_{\text{Mic}} = 342 \text{ m}^2 \text{ g}^{-1}$), whereas the prepared adsorbent material contained only 23% ($S_{\text{Mic}} = 147 \text{ m}^2 \text{ g}^{-1}$) of micropores in its structure. The total pore volume in the prepared charcoal was $0.39 \text{ cm}^3 \text{ g}^{-1}$, of which only $0.09 \text{ cm}^3 \text{ g}^{-1}$ was related to the microporous volume. However, in the commercial adsorbent, the total pore volume was $0.29 \text{ cm}^3 \text{ g}^{-1}$, of which $0.19 \text{ cm}^3 \text{ g}^{-1}$ was related to the micropores. In summary, the prepared charcoal had a higher mesoporous area than the commercial charcoal. This observation is corroborated by the BJH distributions (Fig. 1, inset), in which the mean pore size for both

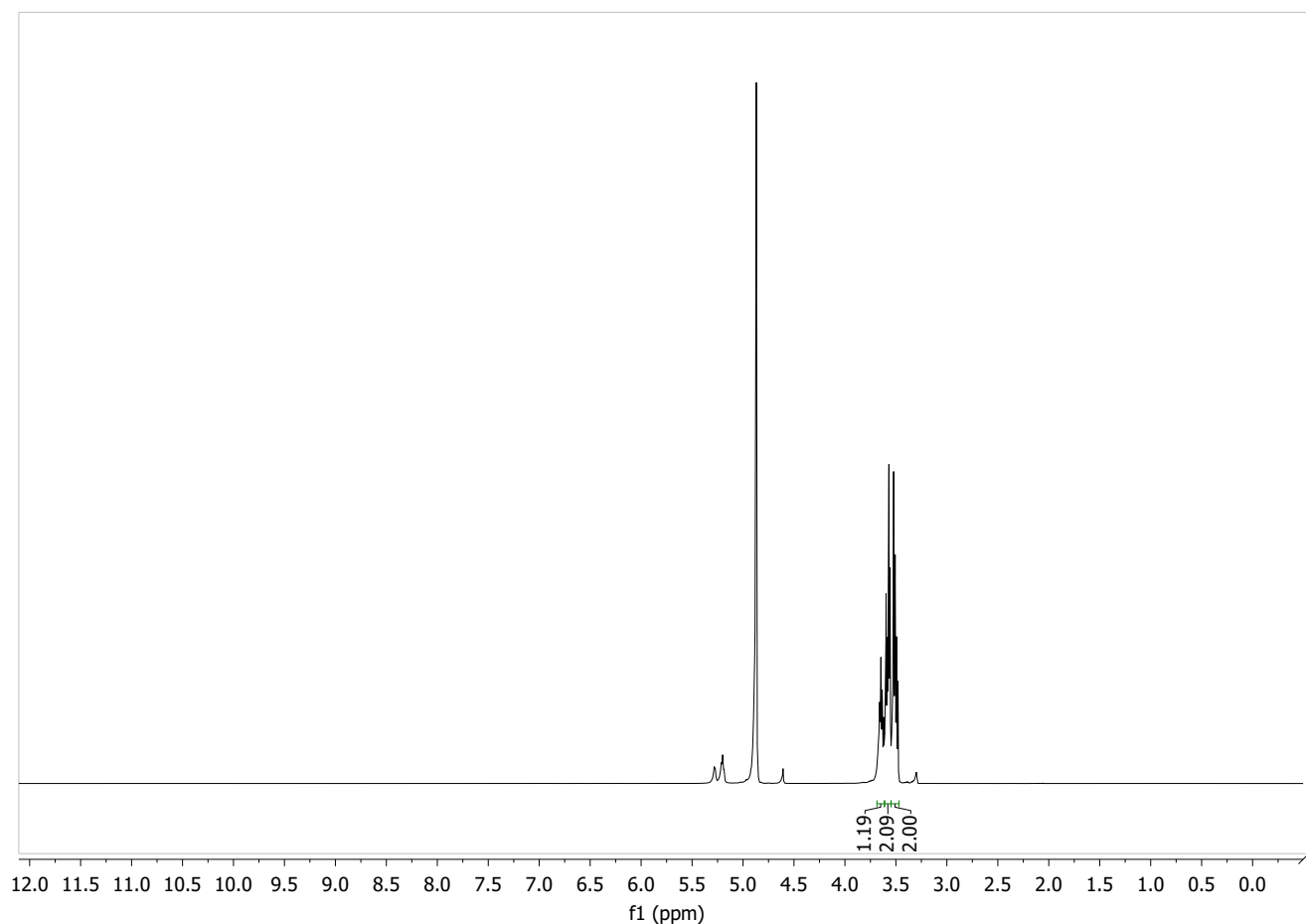


Fig. 2 ^1H -NMR spectrum of purified glycerol

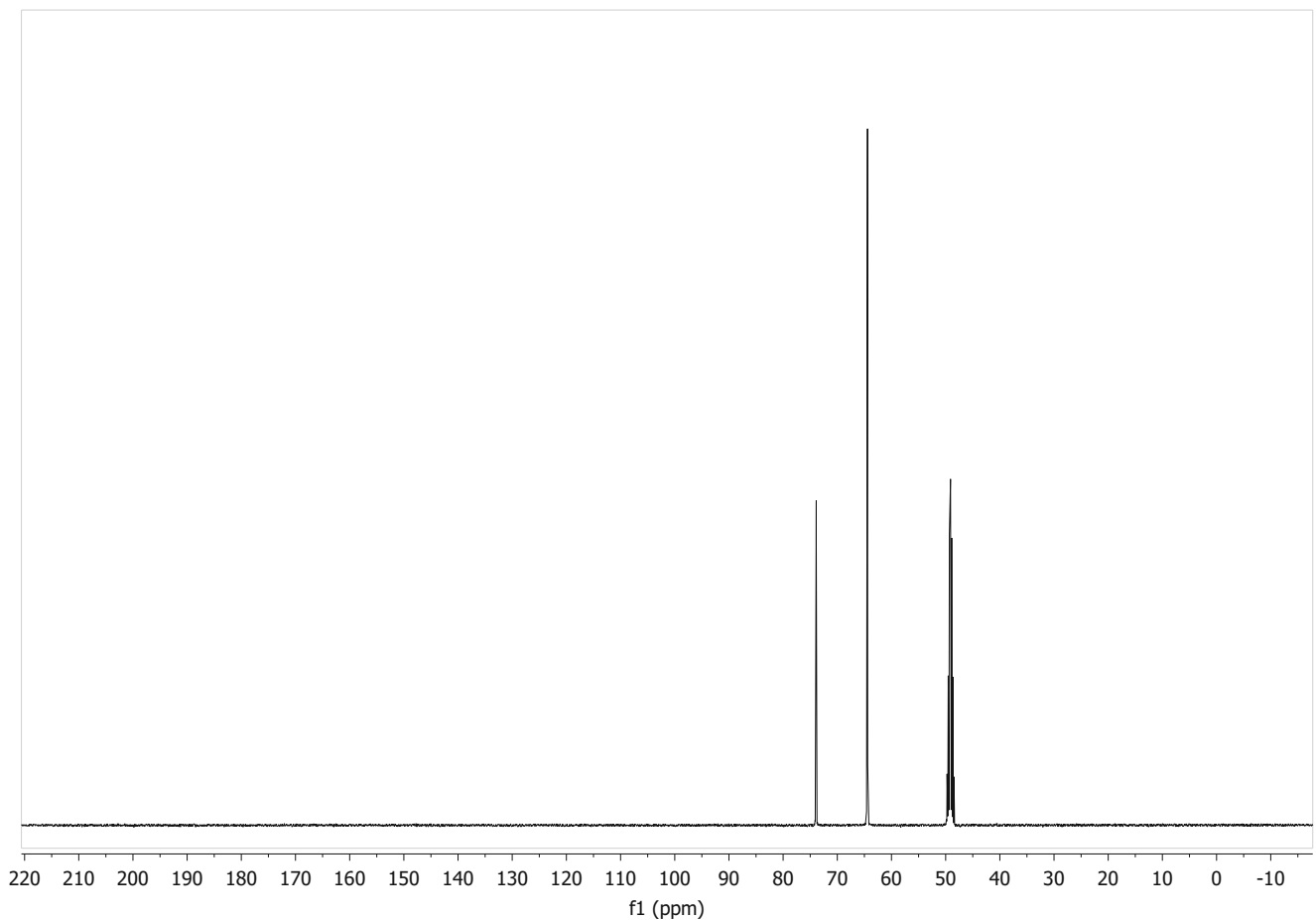
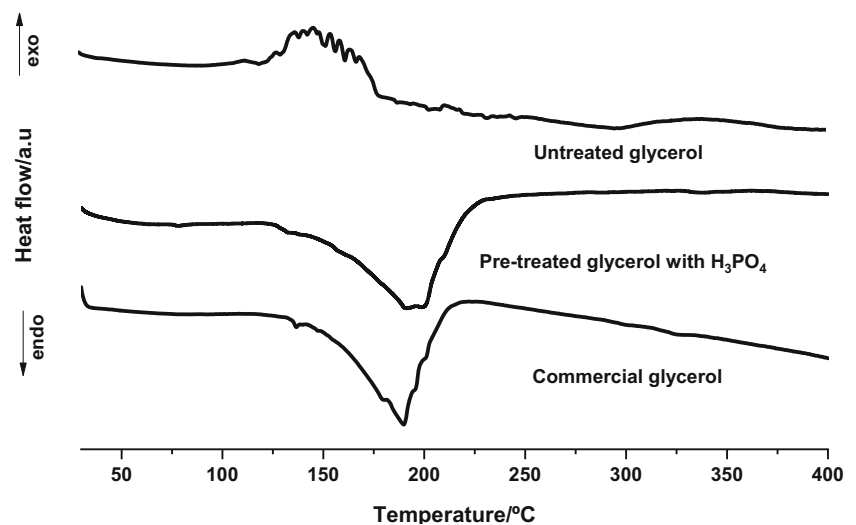


Fig. 3 ^{13}C -NMR spectrum of purified glycerol

samples was shown to be ~ 2.5 nm. However, the curve is wider in the case of prepared charcoal than for the commercial sample. This fact indicates that a large number of mesopores exist on the prepared charcoal, which makes it more suitable for use as an adsorbent in the purification of glycerol than commercial charcoal.

Fig. 4 DSC curves of untreated glycerol, glycerol pretreated with H_3PO_4 , and commercial glycerol, under dynamic nitrogen atmosphere at 50 mL min^{-1} and heating rate of $10 \text{ }^\circ\text{C min}^{-1}$



3.1.2 Acidity of prepared and commercial activated charcoals

The acidities of the prepared and commercial activated charcoals were determined by infrared spectroscopy after adsorption of pyridine by the samples. The areas of the bands at 1545 and 1450 cm^{-1} , characteristic of the interaction between

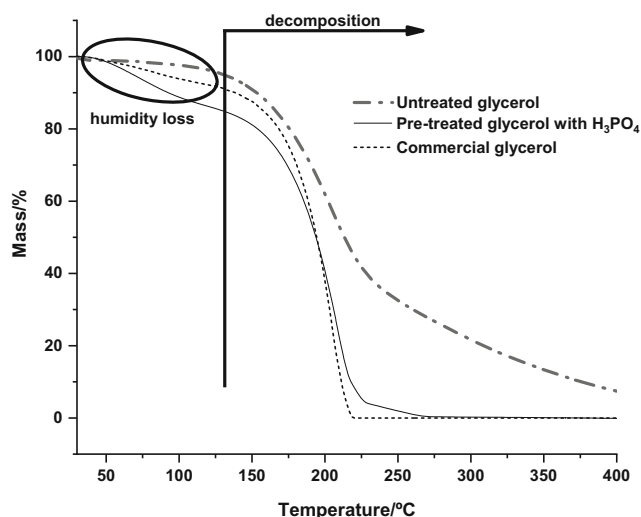


Fig. 5 TG curves of untreated glycerol (thick solid line), glycerol pretreated with H_3PO_4 (thin solid line), and commercial glycerol (dashed line), under dynamic nitrogen atmosphere at 50 mL min^{-1} and heating rate of $10 \text{ }^\circ\text{C min}^{-1}$

pyridine and acid sites, were used to calculate the acidity of each Brønsted and Lewis site, respectively, by means of the equation: $qB, L = (AB, L\pi D^2)(4wEB, L)^{-1}$ where, D is the tablet diameter (cm), w is the sample mass (g), AB, L is the integration of the characteristic band areas (absorbance), EB, L is the extinction coefficient of the pyridine interaction with the Brønsted acid sites = $1.67 \pm 0.12 \text{ cm } \mu\text{mol}^{-1}$ and Lewis acid sites = $2.22 \pm 0.21 \text{ cm } \mu\text{mol}^{-1}$.

Commercial charcoal: Bronsted sites, $183.35 \text{ } \mu\text{mol/g}$; Lewis sites, $264.39 \text{ } \mu\text{mol/g}$; charcoal produced from the macaúba pulp: Bronsted sites, $118.23 \text{ } \mu\text{mol/g}$; Lewis sites, $104.86 \text{ } \mu\text{mol/g}$

Samples-pyridine method-KBr pellets-infrared

Charcoal: $m = 0.0687 \text{ g}$ containing $1.42 \times 10^{-4} \text{ g}$ of commercial charcoal (0.207%), diameter = 0.90 cm, Brønsted area (1545 cm^{-1}), Lewis area (1450 cm^{-1}).

Charcoal produced from the macaúba pulp: $m = 0.0761 \text{ g}$ containing $7.60 \times 10^{-4} \text{ g}$ of the sample (0.998%), diameter = 0.90 cm, Brønsted area (1545 cm^{-1}), and Lewis area (1450 cm^{-1}).

3.1.3 Purification of crude glycerol with activated charcoal

The glycerol obtained from the transesterification of waste cooking was pretreated by filtering the K_3PO_4 formed by the addition of H_3PO_4 to the crude glycerol containing KOH. The activated charcoal prepared from the macaúba residue was used for the adsorptive purification of pretreated CG to remove the pigments, such as β -carotene. The analyses described below demonstrated that the purified glycerol was 95.99% pure. The remaining 4.01% was identified as water by GC and thermal analysis.

The activated charcoal produced from the macaúba endocarp has a larger surface area ($627 \text{ m}^2 \text{ g}^{-1}$) than that of commercial activated charcoal ($470 \text{ m}^2 \text{ g}^{-1}$). It was also more effective for the removal of pigments from crude glycerol than the commercial charcoal. The commercial activated charcoal did not remove all the carotenoid pigments from the glycerol. The vegetable oil contains carotene and chlorophyll. The latter is more extensively degraded during the transesterification than the carotenoids, and the carotene can be carried over to the glycerol. The pigments were more effectively removed by prepared charcoal than by the commercial charcoal because it has a greater mesopore area and might also possess a more active surface. The larger pore size permits the penetration of larger molecules. The commercial charcoal possesses more acid groups than the prepared charcoal. Therefore, its surface might be more polar and have a lower affinity for the carotenoid molecules.

3.1.4 ^1H - and ^{13}C -NMR analysis of the purified glycerol

The high degree of purity of the glycerol obtained using treated charcoal was confirmed by the NMR analyses (Figs. 2 and 3). The signal with a chemical shift at 64.4 ppm in the ^{13}C -NMR spectrum (Fig. 3) corresponds to the methylene carbons of glycerol, and the signal at 63.9 ppm corresponds to the methine carbon.

In Fig. 2, a double doublet (J 4 Hz) centered at 3.50 ppm and a double doublet (J 4 Hz) between 3.54 and 3.60 ppm correspond to the methylene hydrogens of glycerol. The multiplet from 3.62 to 3.68 ppm corresponds to the methine hydrogen. The hydroxyl hydrogens absorbed at 4.8 ppm.

3.1.5 Thermal analysis of the pretreated glycerol and the crude glycerol

The commercial glycerol samples and samples of glycerol treated with H_3PO_4 showed similar enthalpy curves, as can be seen in Fig. 4, where a broad endothermic event between ~ 130 and $230 \text{ }^\circ\text{C}$ corresponding to thermal decomposition can be seen, with almost total mass loss in a single ramp (Fig. 5, glycerol pretreated with H_3PO_4 —thin solid line and commercial glycerol—dashed line). The TG curves indicate a mass loss between ~ 30 and $\sim 120 \text{ }^\circ\text{C}$, corresponding to the moisture. The untreated glycerol decomposes in two stages (Fig. 5, dashed dotted line), which is a characteristic of a complex decomposition mechanism, as previously described [50–54]. This behavior suggests the presence of components that interfere in the process, as expected, because the untreated sample might contain residues from the synthesis. The thermal behavior of untreated glycerol, DSC (Fig. 4) and TG curves (Fig. 5) confirms the presence of synthetic impurities, an aspect to be considered when producing glycerol.

4 Conclusion

We demonstrated that the activated charcoal produced from the macaúba endocarp has a larger surface area ($627 \text{ m}^2 \text{ g}^{-1}$) than that of commercial activated charcoal ($470 \text{ m}^2 \text{ g}^{-1}$). It was also more effective for the removal of pigments from crude glycerol than the commercial charcoal. The method employed using only filtration through activated charcoal after the pretreatment with phosphoric acid to remove the KOH furnished glycerol of 95.99% purity.

Funding information The authors acknowledge the financial support and scholarships furnished by the CNPq, FAPEMIG and financed in part by the Coordenação de Aperfeiçoamento de Pessoal de Nível Superior-Brasil (CAPES), Finance Code 001.

References

- Zahan KA, Kano M (2017) biodiesel production from palm oil, its by-products, and mill effluent: a review. *Energies*. <https://www.mdpi.com/1996-1073/11/8/2132/pdf>
- Wang T (2019) Global biodiesel production by country. *Statista*. <https://www.statista.com/statistics/274168/biofuel-production-in-leading-countries-in-oil-equivalent/>
- Knoema Enterprise Data Solutions (2017) Biodiesel production. <https://knoema.com/atlas/topics/Energy/Renewables/Biodiesel-production>. Accessed 10 Apr 2020
- United States Energy Information Administration (2020) Biodiesel Production by Country. <https://www.indexmundi.com/energy/?product=biodiesel&graph=production&display=rank>
- Gupta M, Kumar N (2012) Scope and opportunities of using glycerol as an energy source. *Renew Sust Energ Rev* 16:4551–4556. <https://doi.org/10.1016/j.rser.2012.04.001>
- Quispe CAG, Coronado CJR, Carvalho JA Jr (2013) Glycerol: production, consumption, prices, characterization and new trends in combustion. *Renew Sust Energ Rev* 27:475–493. <https://doi.org/10.1016/j.rser.2013.06.017>
- Baba Y, Tada C, Watanabe R, Fukuda Y, Chida N, Nakai Y (2013) Anaerobic digestion of crude glycerol from biodiesel manufacturing using a large-scale pilot plant: methane production and application of digested sludge as fertilizer. *Bioresour Technol* 140:342–348. <https://doi.org/10.1016/j.biortech.2013.04.020>
- Surendra KC, Sawatdeenarunat C, Shrestha S, Sung S, Khanal SK (2015) Anaerobic digestion-based biorefinery for bioenergy and biobased products. *Ind Biotechnol* 11:103–112. <https://doi.org/10.1089/ind.2015.0001>
- Zijlstra RT, Beltranena E (2013) Swine convert co-products from food and biofuel industries into animal protein for food. *Animal Frontiers* 3:48–53. <https://doi.org/10.2527/af.2013-0014>
- González R, Smith R, Blanco D, Fierro J, Gómez X (2019) Application of thermal analysis for evaluating the effect of glycerine addition on the digestion of swine manure. *J Therm Anal Calorim* 135:2277–2286. <https://doi.org/10.1007/s10973-018-7464-8>
- Pott RWM, Howe CJ, Dennis JS (2014) The purification of crude glycerol derived from biodiesel manufacture and its use as a substrate by *Rhodopseudomonas palustris* to produce hydrogen. *Bioresour Technol* 152:464–470. <https://doi.org/10.1016/j.biortech.2013.10.094>
- Mota CJA, Peres Pinto B, de Lima AL (2017) A versatile renewable feedstock for the chemical industry. Chapter 2. Glycerol utilization. <https://www.springer.com/gp/book/9783319593746>
- Vivek N, Pandey A, Binod P (2015) Biological valorization of pure and crude glycerol into 1,3-propanediol using a novel isolate *Lactobacillus brevis* N1E9.3.3. *Bioresour Technol*. <https://doi.org/10.1016/j.biortech.2016.02.020>
- Isahak WNRW, Ismail M, Yarmo MA, Jahim JM, Salimon J (2010) Purification of crude glycerol from transesterification RBD palm oil over homogeneous and heterogeneous catalysts for the biolubricant preparation. *J Appl Sci* 10:2590–2595. <https://doi.org/10.3923/jas.2010.2590.2595>
- Konstantinovic S, Danilovic B, Ciric J et al (2016) Valorization of crude glycerol from biodiesel production. *Chem Ind Chem Eng Q* 22:461–489. <https://doi.org/10.2298/CICEQ160303019K>
- Yang F, Hanna MA, Sun R (2012) Value-added uses for crude glycerol—a byproduct of biodiesel production. *Biotechnol Biofuels* 5:13. <https://doi.org/10.1186/1754-6834-5-13>
- Chen J, Yan S, Zhang X, Tyagi RD, Surampalli RY, Valéro JR (2018) Chemical and biological conversion of crude glycerol derived from waste cooking oil to biodiesel. *Waste Manag* 71:164–175. <https://doi.org/10.1016/j.wasman.2017.10.044>
- García-Martín JF, Alés-Álvarez FJ, Torres-García M, Feng C-H, Álvarez-Mateos P (2019) Production of oxygenated fuel additives from residual glycerine using biocatalysts obtained from heavy-metal-contaminated *Jatropha curcas* L. Roots. *Energies*. <https://www.mdpi.com/1996-1073/12/4/740>, Production of Oxygenated Fuel Additives from Residual Glycerine Using Biocatalysts Obtained from Heavy-Metal-Contaminated *Jatropha curcas* L. Roots
- Manosak R, Limpattayanate S, Hunsom M (2011) Sequential-refining of crude glycerol derived from waste used-oil methyl ester plant via a combined process of chemical and adsorption. *Fuel Process Technol* 92:92–99. <https://doi.org/10.1016/j.fuproc.2010.09.002>
- Delample M, Villandier N, Douliez J-P, Camy S, Condoret J-S, Pouilloux Y, Barrault J, Jérôme F (2010) Glycerol as a cheap, safe and sustainable solvent for the catalytic and regioselective β , β -diarylation of acrylates over palladium nanoparticles. *Green Chemistry*. <https://pubs.rsc.org/en/Content/ArticleLanding/GC/2010/B925021B#!divAbstract>
- Hansen CF, Hernandez A, Mullan BP, Moore K, Trezona-Murray M, King RH, Pluske JR (2009) A chemical analysis of samples of crude glycerol from the production of biodiesel in Australia, and the effects of feeding crude glycerol to growing-finishing pigs on performance, plasma metabolites and meat quality at slaughter. *Anim Prod Sci* 49:154. <https://doi.org/10.1071/ea08210>
- Thompson JC, He BB (2006) Characterization of crude glycerol from biodiesel production from multiple feedstocks. *Appl Eng Agric* 22:261–265. <https://doi.org/10.13031/2013.20272>
- Frimmel FH, Noble RD, Terry PA (2005) Principles of chemical separations with environmental applications. *Angew Chem* 117: 187–188. <https://doi.org/10.1002/ange.200485210>
- Van Gerpen J (2005) Biodiesel processing and production. *Fuel Process Technol* 86:1097–1107. <https://doi.org/10.1016/j.fuproc.2004.11.005>
- Dzyazko YS, Rozhdestvenska LM, Vasilyuk SL, Kudelko KO, Belyakov VN (2017) Composite membranes containing nanoparticles of inorganic ion exchangers for electro-dialytic desalination of glycerol. *Nanoscale Res Lett* 12:438. <https://doi.org/10.1186/s11671-017-2208-4>
- Isahak WNRW, Ismail M, Yarmo MA, Jahim JM, Salimon J (2010) Purification of crude glycerol from transesterification RBD palm oil over homogeneous and heterogeneous catalysts for the biolubricant preparation. *Journal of Applied Sciences*. <https://scialert.net/abstract/?doi=jas.2010.2590.2595>, Purification of Crude Glycerol

- from Transesterification RBD Palm Oil over Homogeneous and Heterogeneous Catalysts for the Biolubricant Preparation
27. Carmona M, Valverde JL, Perez A, Warcholb J, Rodríguez JF (2009) Purification of glycerol/water solutions from biodiesel synthesis by ion exchange: sodium removal Part I. *J Chem Technol; Biotechnol.* <https://doi.org/10.1002/jctb.2106>
 28. Saleh J, Tremblay AY, Dubé MA (2010) Glycerol removal from biodiesel using membrane separation technology. *Fuel.* 89:2260–2266. <https://doi.org/10.1016/j.fuel.2010.04.025>
 29. Kongjao S, Damronglerd S, Hunsom M (2010) Purification of crude glycerol derived from waste used-oil methyl ester plant. *Korean J Chem Eng* 27:944–949. <https://doi.org/10.1007/s11814-010-0148-0>
 30. Isahak W, Che Ramli ZA, Ismail M, et al (2014) Recovery and purification of crude glycerol from vegetable oil transesterification: a review. *Sep Purif Rev.* <https://doi.org/10.1080/15422119.2013.851696>
 31. Xiao Y, Xiao G, Varma A, Isahak WW (2013) A universal procedure for crude glycerol purification from different feedstocks in biodiesel production: experimental and simulation study. *Ind Eng Chem Res* 52:14291–14296. <https://doi.org/10.1021/ie402003u>
 32. Ardi MS, Aroua MK, Hashim NA (2015) Progress, prospect and challenges in glycerol purification process: a review. *Renew Sust Energ Rev* 42:1164–1173. <https://doi.org/10.1016/j.rser.2014.10.091>
 33. Turk Sekulić M, Pap S, Stojanović Z, Bošković N, Radonić J, Šolević Knudsen T (2018) Efficient removal of priority, hazardous priority and emerging pollutants with Prunus armeniaca functionalized biochar from aqueous wastes: experimental optimization and modeling. *Sci Total Environ* 613-614:736–750. <https://doi.org/10.1016/j.scitotenv.2017.09.082>
 34. Alves CCO, Faustino MV, Franca AS, Oliveira LS (2014) Comparative evaluation of activated carbons prepared by thermochemical activation of lignocellulosic residues in fixed bed column studies. *Int J Eng Technol* 7:465–469. <https://doi.org/10.7763/ijet.2015.v7.838>
 35. Yakout SM, Sharaf El-Deen G (2016) Characterization of activated carbon prepared by phosphoric acid activation of olive stones. *Arab J Chem* 9:S1155–S1162. <https://doi.org/10.1016/j.arabjc.2011.12.002>
 36. Zhu Z, Liu Z, Liu S, Niu H, Hu T, Liu T, Xie Y (2000) NO reduction with NH₃ over an activated carbon-supported copper oxide catalysts at low temperatures. *Appl Catal B Environ* 26:25–35. [https://doi.org/10.1016/S0926-3373\(99\)00144-7](https://doi.org/10.1016/S0926-3373(99)00144-7)
 37. Acosta R, Fierro V, Martínez de Yuso A, Nabarlart D, Celzard A (2016) Tetracycline adsorption onto activated carbons produced by KOH activation of tyre pyrolysis char. *Chemosphere.* 149:168–176. <https://doi.org/10.1016/j.chemosphere.2016.01.093>
 38. Elmouwahidi A, Zapata-Benabite Z, Carrasco-Marín F, Moreno-Castilla C (2012) Activated carbons from KOH-activation of argan (*Argania spinosa*) seed shells as supercapacitor electrodes. *Bioresour Technol* 111:185–190. <https://doi.org/10.1016/j.biortech.2012.02.010>
 39. Ubago-Pérez R, Carrasco-Marín F, Fairén-Jiménez D, Moreno-Castilla C (2006) Granular and monolithic activated carbons from KOH-activation of olive stones. *Microporous Mesoporous Mater* 92:64–70. <https://doi.org/10.1016/j.micromeso.2006.01.002>
 40. Byamba-Ochir N, Shim WG, Balathanigaimani MS, Moon H (2016) Highly porous activated carbons prepared from carbon rich Mongolian anthracite by direct NaOH activation. *Appl Surf Sci* 379:331–337. <https://doi.org/10.1016/j.apsusc.2016.04.082>
 41. Islam MA, Ahmed MJ, Khanday WA, Asif M, Hameed BH (2017) Mesoporous activated carbon prepared from NaOH activation of rattan (*Lacosperma secundiflorum*) hydrochar for methylene blue removal. *Ecotoxicol Environ Saf* 138:279–285. <https://doi.org/10.1016/j.ecoenv.2017.01.010>
 42. Ternero-Hidalgo JJ, Rosas JM, Palomo J, Valero-Romero MJ, Rodríguez-Mirasol J, Cordero T (2016) Functionalization of activated carbons by HNO₃ treatment: influence of phosphorus surface groups. *Carbon N Y* 101:409–419. <https://doi.org/10.1016/j.carbon.2016.02.015>
 43. Shamsuddin MS, Yusoff NRN, Sulaiman MA (2016) Synthesis and characterization of activated carbon produced from kenaf core fiber using H₃PO₄ activation. *Procedia Chem* 19:558–565. <https://doi.org/10.1016/j.proche.2016.03.053>
 44. Giraldo L, Ladino Y, Piraján JCM, Rodríguez MP (2007) Synthesis and characterization of activated carbon fibers from Kevlar. *Ecletica Quim* 32:55–62. <https://doi.org/10.1590/S0100-46702007000400008>
 45. Yorgun S, Yildiz D (2015) Preparation and characterization of activated carbons from Paulownia wood by chemical activation with H₃PO₄. *J Taiwan Inst Chem Eng* 53:122–131. <https://doi.org/10.1016/j.jtice.2015.02.032>
 46. Kumar A, Jena HM (2017) Adsorption of Cr(VI) from aqueous phase by high surface area activated carbon prepared by chemical activation with ZnCl₂. *Process Saf Environ Prot* 109:63–71. <https://doi.org/10.1016/j.psep.2017.03.032>
 47. Demiral İ, Aydın Şamdan C, Demiral H (2016) Production and characterization of activated carbons from pumpkin seed shell by chemical activation with ZnCl₂. *Desalin Water Treat* 57:2446–2454. <https://doi.org/10.1080/19443994.2015.1027276>
 48. Khenniche L, Benissad-Aissani F (2010) Adsorptive removal of phenol by coffee residue activated carbon and commercial activated carbon: equilibrium, kinetics, and thermodynamics. *J Chem Eng Data* 55:4677–4686. <https://doi.org/10.1021/je100302e>
 49. Komintarachat C, Chuepeng S (2010) Methanol-based transesterification optimization of waste used cooking oil over potassium hydroxide catalyst. *Am J Appl Sci* <https://pdfs.semanticscholar.org/407c/0888dd132d6b831086d581a6d1153d5d778c.pdf> 7:1073–1078
 50. Barbosa SL, Ottone M, Santos MC, Junior GC, Lima CD, Glososki GC, Lopes NP, Klein SI (2015) Benzyl benzoate and dibenzyl ether from benzoic acid and benzyl alcohol under microwave irradiation using a SiO₂-SO₃H catalyst. *Catal Commun* 68:97–100. <https://doi.org/10.1016/j.catcom.2015.04.033>
 51. Moreno-Castilla C (2004) Adsorption of organic molecules from aqueous solutions on carbon materials. *Carbon.* 42:83–94. <https://doi.org/10.1016/j.carbon.2003.09.022>
 52. Marques MBF, Araujo BCR, Fernandes C, Yoshida MI, Mussel WN, Sebastião RCO (2020) Kinetics of lumefantrine thermal decomposition employing isoconversional models and artificial neural network. *J Braz Chem Soc.* <https://doi.org/10.21577/0103-5053.20190211>
 53. Brito LG, Leite GQ, Duarte FÍC, Ostrosky EA, Ferrari M, de Lima AAN, Nogueira FHA, Aragão CFS, de Lelis Ferreira BD, de Freitas Marques MB, Yoshida MI, Mussel WN, Sebastião RCO, Gomes APB (2019) Thermal behavior of ferulic acid employing isoconversional models and artificial neural network. *J Therm Anal Calorim* 138:3715–3726. <https://doi.org/10.1007/s10973-019-08114-x>
 54. Ferreira BDL, Araújo NRS, Ligório RF, Pujatti FJP, Mussel WN, Yoshida MI, Sebastião RCO (2018) Kinetic thermal decomposition studies of thalidomide under non-isothermal and isothermal conditions. *J Therm Anal Calorim* 134:773–782. <https://doi.org/10.1007/s10973-018-7568-1>

Publisher's note Springer Nature remains neutral with regard to jurisdictional claims in published maps and institutional affiliations.

Affiliations

Sandro L. Barbosa¹  · Milton S. de Freitas¹  · Wallans T. P. dos Santos¹ · David Lee Nelson¹ · Maria Betânia de Freitas Marques¹ · Stanlei I. Klein² · Giuliano C. Clososki³ · Franco J. Caires³  · Eduardo J. Nassar⁴ · Lucas D. Zanatta⁵ · Foster A. Agblevor⁶ · Carlos A. M. Afonso⁷ · Adriano C. Moraes Baroni⁸

¹ Department of Pharmacy, Universidade Federal dos Vales do Jequitinhonha e Mucuri-UFVJM, Campus JK, Rodovia MGT 367-Km 583, N° 5000, Alto da Jacuba, Diamantina, MG CEP 39100-000, Brazil

² Department of General and Inorganic Chemistry, Institute of Chemistry, São Paulo State University-Unesp, R. Prof. Francisco Degni 55, Quitandinha, Araraquara, SP CEP-14.800-900, Brazil

³ Department of Physics and Chemistry, Faculdade de Ciências Farmacêuticas de Ribeirão Preto, São Paulo University-USP, Av. Do Café s/n, Ribeirão Preto, SP CEP-14.040-903, Brazil

⁴ Universidade de Franca, Av. Dr. Armando Sales Oliveira, 201, C.P. 82, Franca, SP CEP-10404-600, Brazil

⁵ Laboratório de Química Bioinorgânica, Departamento de Química, Faculdade de Filosofia, Ciências e Letras de Ribeirão Preto, Universidade de São Paulo, Av. Bandeirantes, 3900, Ribeirão Preto, SP 14040-901, Brazil

⁶ USTAR Bioenergy Center, Biological Engineering, Utah State University, Logan, UT 84322, USA

⁷ Research Institute for Medicines (iMed.Ulisboa), Faculty of Pharmacy, Universidade de Lisboa, Av. Prof. Gama Pinto, 1649-003 Lisbon, Portugal

⁸ Faculdade de Ciências Farmacêuticas, Alimentos e Nutrição, Universidade Federal de Mato Grosso do Sul-UFMS, Av. Costa e Silva, s.n, Campo Grande, MS 79070900, Brazil